IOP Conf. Series: Materials Science and Engineering **101** (2015) 012119 doi:10.1088/1757-899X/101/1/012119

Qualification of Fin-Type Heat Exchangers for the ITER Current Leads

A Ballarino[4], P Bauer[1 *], B Bordini[4], A Devred[1], K Ding[2], E Niu[3], M Sitko[4], T Taylor[5], Y Yang[6], T Zhou[2]

[1]ITER Organization, Route de Vinon sur Verdon, CS90046, 13067 St. Paul lez Durance Cedex, France
[2]Institute for Plasma Physics of the Chinese Academy of Sciences Hefei, Anhui (230031), China
[3]China International Nuclear Fusion Energy Program Execution Center Beijing 100862, China
[4]CERN - European Center for Particle Physics 1217 Meyrin, Switzerland
[5]AT Scientific LLC 1233 Bernex, Switzerland
[6]Institute of Cryogenics, University of Southampton Southampton SO17 1BJ, United Kingdom

E-mail: pierre.bauer@iter.org

Abstract. The ITER current leads will transfer large currents of up to 68 kA into the biggest superconducting magnets ever built. Following the development of prototypes and targeted trials of specific manufacturing processes through mock-ups, the ASIPP (Chinese Institute of Plasma Physics) is preparing for the series fabrication. A key component of the ITER HTS current leads are the resistive heat exchangers. Special R&D was conducted for these components at CERN and ASIPP in support of their designs. In particular several mock-ups were built and tested in room temperature gas to measure the dynamic pressure drop and compare to 3D CFD models.

1. Introduction

The Current Leads (CL) are key components of the ITER superconducting magnet system. The CLs provide the cold/warm transitions for the large currents fed to the ITER superconducting coils from the warm power supply and distribution system. By using hybrid High-Temperature Superconductor (HTS) / resistive copper leads, the heat load into the cryogenic system at the cold end of the leads can be reduced by a factor of up to five with respect to fully resistive leads. Resulting savings on cost of operation more than compensate for the extra cost of manufacture. ITER requires a total of 60 current leads, 18 for the TF coil system, 12 for the CS coil system, 12 for the PF coil system and 18 for the correction coil system, with a total current capacity of approximately 2.6 MA.

* To whom any correspondence should be addressed.

Content from this work may be used under the terms of the Creative Commons Attribution 3.0 licence. Any further distribution of this work must maintain attribution to the author(s) and the title of the work, journal citation and DOI.
Published under licence by IOP Publishing Ltd

Following the first successful large scale application of HTS current leads using Bi2223 superconductor in CERN's LHC project [1], a "demonstrator prototype" for these current leads was built and tested at KIT (Karlsruhe Institute of Technology) in 2002-2006 [2]. The demonstrator verified the basic design concepts discussed below and confirmed the choice of 50 K as supply temperature for the cooling of the resistive heat exchanger. After the decision to entrust the Chinese ITER party with the in-kind contribution of the ITER current leads, ASIPP (the Institute for Plasma Physics) in 2009 and 2010 undertook the manufacturing and testing of the first pre-prototypes [3], [4]. ITER then released the final designs of the three types of CLs in 2011 [5].

The hybrid design of the ITER current leads consists of a copper heat exchanger section, covering the temperature range from 300 K to 65 K, and a superconducting section, covering the 65 K to 4.5 K range. The resistive heat exchanger design is scaled from that of the LHC HTS current leads: it is a fin-type, cooled with zig-zag counter-flow of GHe, which enters at 50 K and 0.4 MPa and exits at the warm terminal at about 300 K. The HTS section between 5 K and 65 K, which uses Bi-2223 superconductor tapes with a gold-doped silver matrix, is conduction-cooled from the bottom end, which in turn is cooled by a flow of supercritical helium at ~5-6 K, 0.5-0.6 MPa.

Following the development of the CL designs, a multi-step qualification program was launched in ASIPP, including mock-ups [6,7] and prototypes (now being tested), each of these having to be completed successfully before fabrication of the leads proper could commence. Also included in the qualification program were two mock-ups of the resistive heat exchanger, one of the CC type (10 kA) and another of the TF type (68 kA).

The heat exchanger is the most complex and thus the key component of the HTS leads. In this paper we discuss in detail the experiences gained during the qualification process for these heat exchanger mock-ups, including the testing at ASIPP and CERN, and the cross-check against computer models.

2. Heat Exchanger for the ITER Current Leads

The optimization of the HX aims at minimizing the helium mass flow rate required for its cooling in nominal operating conditions. For the modelling, this corresponds to imposing to the temperature profile a zero gradient at the room temperature end, in which case all the heat generated by Joule heating along the copper rod is transferred into the helium flow. At the same time, the geometry of the heat exchanger must assure the required heat exchange surface and heat exchange efficiency. The strong temperature dependence of material properties must be taken into account in the optimization. The following five aspects of the HX affect cooling mass flow and safety requirements: 1) high efficiency, 2) sufficient time before thermal runaway in the so-called LOFA ("Loss of Flow Accident"), 3) optimum dimensions (length to cross-section ratio) for minimizing conductive heat in-flow, 4) reasonably low pressure drop ($\leq$ 1.5 bar), and 5) low resistance of the connection to the HTS module (and to the warm terminal). The design of the heat exchangers is discussed in the following.

2.1. Heat Exchanger Design

The HX for the 68 kA TF-type current lead is illustrated in figure 1. The cooling helium gas is confined to follow the zigzag path along the HX by the enveloping, stainless steel tube that is tightly fitted over the HX core. An advantage of this fin-type design, especially for a larger production, is that quality of assembly and therefore performance can be controlled via a detailed geometrical survey (as opposed to extensive testing as performed here in the frame of the qualification program). Although most of the leads are of the pulsed type (the only exception is the TF lead), it was decided to optimize the heat exchanger designs for DC operation at the peak current of the electrical cycle. This is a

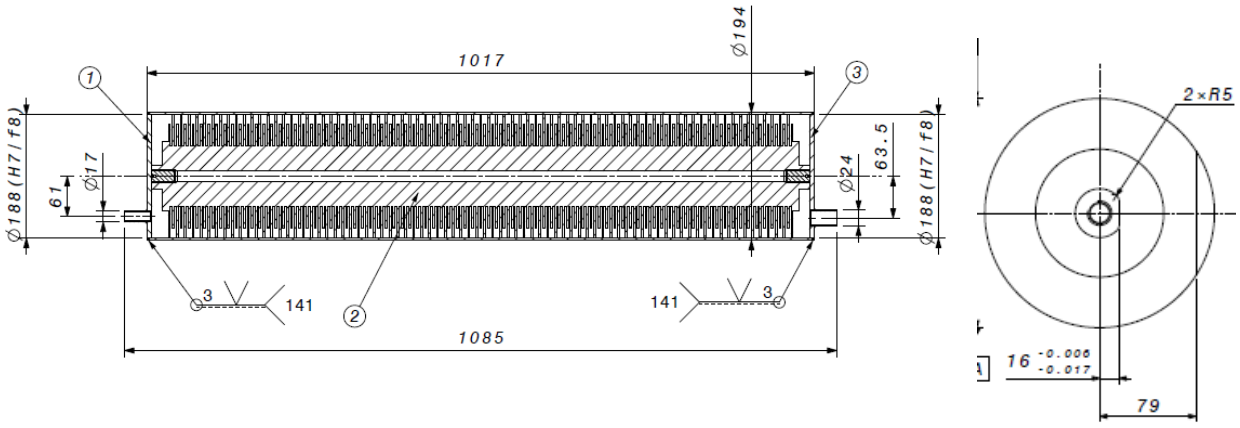

Figure 1. Design of HX for the 68 kA (TF-type) lead

conservative and thus safe approach, but justified, given the large stored energy of the ITER magnet system transported through these leads. The design current and the main geometrical parameters are summarized in table 1. The fin thickness is 3 mm, as is the spacing between fins. The length is the total length of the heat exchanger measured between the end fins; the cut dimension in the table is the depth of the segment that is removed from alternating sides to permit zig-zag flow. As for the LHC leads, the central hole of diameter 16 mm (10 mm in the CC-type) is a channel serving as a conduit for the instrumentation wires. Following the method first developed for the LHC current leads, electron beam welding technology is chosen for joining the HX to the room temperature terminal at the warm end, and to the transition section and HTS module at the cold end. This ensures excellent electrical and mechanical connection of the components and uniform quality can be ensured by industrial QC.

Table 1. Dimensions of the heat exchangers of the ITER leads. The cut is the segment cut from the edge of the fin to allow helium to pass (see figure 1). Cuts are on alternating sides of the HX.

Lead type	Design Current	Length (mm)	Fin Ø (mm)	Core Ø (mm)	Cut (mm)	Ø central hole (mm)
CC	10 kA	903	110	38	10	10
PF/CS	55 kA	951	174	82.6	13	16
TF	68 kA	951	188	92.4	15	16

2.2. Manufacturing Approach

The defined assembly tolerance H7/g6 between the HX core and the external sleeve is important for the current lead performance, as it minimizes the amount of gas bypassing the HX core. Another is maintaining the straightness of the HX core during machining. The CC HX core, for example, sags under its own weight by about 0.2 mm. The TF-type HX is machined in less than a week on a 5-axis CNC machine with a straightness deviation of less than 70 microns over 1 m. The complete dimensional survey of the HX core in a Coordinate Measurement Machine (CMM) takes about one day. The diameter of the sleeve in the TF–type CL is required to be less than 70 µm greater than that of the 188 mm diameter HX core. The sleeve is honed to achieve these tight tolerances on the diameter, shape and surface finish. Special tooling was prepared to facilitate the precision checking of its final dimensions. Special tooling was also developed to slide the sleeve over the HX. Before

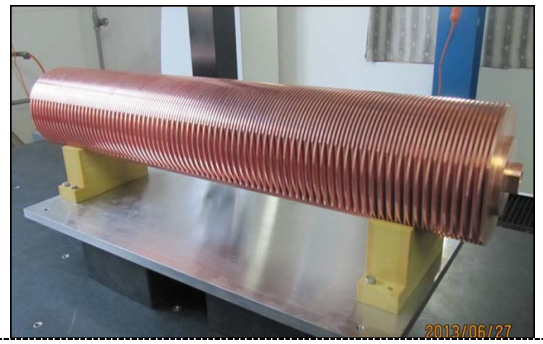

Figure 2. TF-type HX mock-up in the CMM at Juneng

assembly the honed tube is heated to about 180 ℃, increasing its diameter by 0.25 mm for the CC-type HX, and 0.43 mm for TF-type HX. Then the tube is more or less manually slid over the HX core. This operation usually does not take more than 10 seconds. Then the tube is welded in place.

2.3. Heat Exchanger Mock-ups

Two different HX mock-ups were manufactured by two Chinese suppliers, Juneng (TF-type, figure 2) and Keye (CC type), under the supervision of ASIPP. The fabrication and test of the mock-ups was the first step of the qualification of the manufacturing procedures, which was completed with the fabrication of the HX for the prototype leads.

3. Mock up Experiments

3.1. Pressure Drop Tests

Pressure drop tests with Nitrogen (GN2) gas at room temperature were performed on the mock-up copper HX of the current leads in ASIPP (GN2). In combination with calibrated CFD models the measured pressure drops can give information about the amount of bypass-flow. Pressure taps were mounted at the opposite ends and along the HX (with the capillaries perforating the honed tube). The taps were distributed uniformly along the length so that each pair of adjacent taps covers about a quarter of HX length. Differential pressure gauges of several different Full Scales (FS) were purchased to cover a range from 0.1 kPa to 100 kPa. The mass flow rate was measured downstream of the outlet using a fully-opened, calibrated flow controller from Hastings (for measurements below 3 g/s) and the ASIPP flow controller of 5 g/s FS had to be used for a few points above 3.5g/s despite the doubts in its calibration. The test consisted of measurements taken at different inlet pressures and nitrogen flow rates. The quality of the data was checked in-line by comparing the sum of pressure drops of the sub-sections with that measured with the differential gage covering the entire mock-up. Especially for low flow-rates at the limit of the resolution of the differential pressure gages it was useful to plot the data in a log scale (as shown in figure 3) to follow the transition from laminar to turbulent regime. In some cases the gages had to be exchanged for higher resolution, smaller FS gages to correctly measure these points.

Collapsing the data for different inlet pressures using $P_{in}\Delta P$ in log-log scales (figure 3) reveals that the pressure drop obtained correctly scales into a common line. In the turbulent regime, $P_{in}\Delta P$ showed a consistent scaling for both CC and TF type HX, with the transition from laminar to turbulent flow at

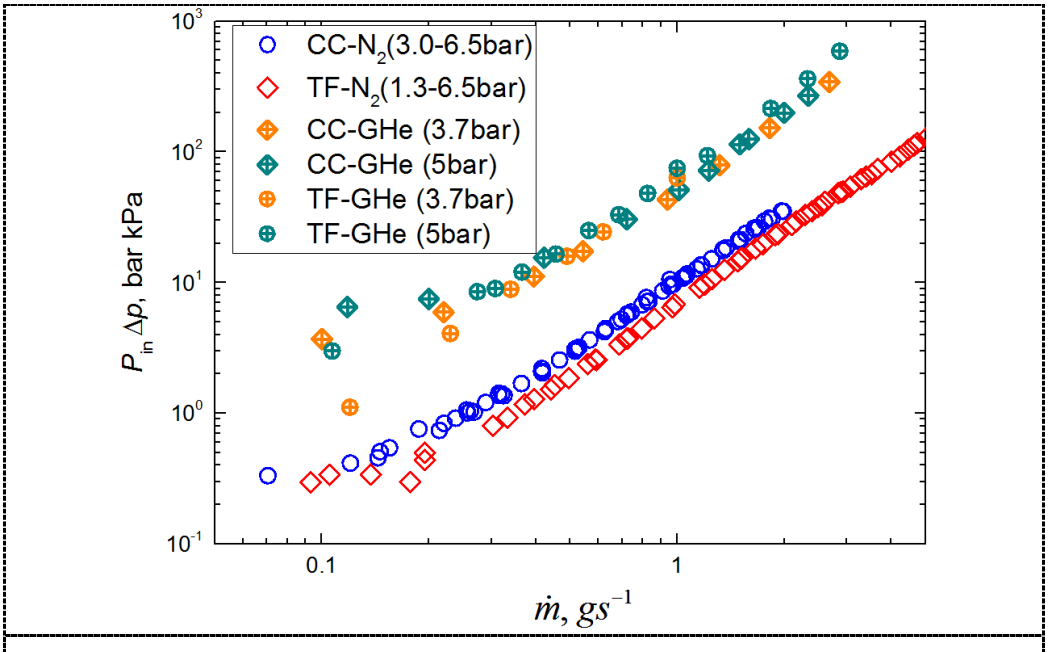

Figure 3. Comparison of $P_{in}\Delta P$ vs flow rate for CC and TF mock-ups

$\dot{m}_c$~0.3 g/s for the CC-type HX and $\dot{m}_c$~0.4 g/s for the TF type HX. The figure also shows a lower pressure drop in TF (by a factor of ~1.8) at a given mass flow rate. It is also noted that both HX have a similar behaviour in turbulence with $P_{in}\Delta P \sim \dot{m}^{1.85}$.

Similar measurements, with matching results, were also performed at CERN, further confirming the quality of these experimental data. CERN also performed tests using Helium (GHe). The data for these tests are also included in figure 3. As expected the GHe and GN2 ΔP data for a given type of HX at the same mass flow rate $\dot{m}$ differ by the inverse ratio of the densities ρ (here a factor 7).

4. Model

To support the HX design effort, a 3D numerical model was prepared using the Comsol Multiphysics® isothermal flow module. Reynolds-averaged Navier-Stokes (RANS) equations together with the k-ε turbulence model are used to represent the turbulent flow. The model couples complex phenomena interacting with each other such as Joule heating, fluid flow and heat transfer by conduction and convection, and uses material and gas temperature dependent properties [8]. The model can now be used to cross-check against the experimental data from the HX mock-ups.

4.1. CFD Modelling of pressure drop

To develop a complex 3D FEM model and optimize the mesh quality a reduced length model was built, consisting of a 6 cm long section (5 meanders of the HX), which represents 1/15th part of a 10 kA HX and 1/16th part of 68 kA HX respectively. Additionally, the inlet and the outlet gas parts in both cases have been extended by 3 cm to avoid entrance effects causing convergence problems. The geometry of the 10 kA (CC) short model is represented in figure 4.

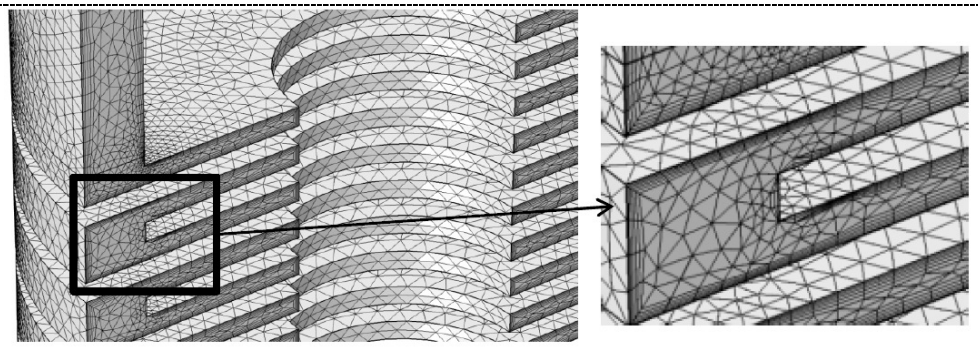

Figure 4. CC-type HX mesh with boundary layers and corner refinement

The simulations were carried out for different mesh configurations The best results were obtained by using the physics-controlled mesh; this type of mesh is characterized by 5 boundary layers, corner refinement and surface meshes that are more accurate than volume meshes. Such a mesh requires approximately 5 million elements and 8 million degrees of freedom (for the $1/16^{th}$ model of the HX). Reasonably good results (3.58% relative error) with a limited number of degree of freedom (0.93 millions) were obtained by using physics-controlled mesh with a predefined 'normal' level of accuracy and reducing the number of boundary layer to 3. However, the results with the best accuracy were given by physics-controlled meshes with an increased number of elements. By comparing the results of such meshes with varying number of elements we can reasonably conclude that the results would not significantly change by further increasing the number of elements.

4.2. Pressure Drop Calculation

Based on the above considerations, the physics-controlled normal mesh with 3 boundary layers has been chosen to simulate the flow of room temperature N2 gas in the full length isothermal model of the 10 kA HX (see figure 5). The model has 8.6 million degrees of freedom, which is almost at the limit of the computing power. From the short model study the expected error from that limited mesh quality is 4.3 %. The simulation results are nevertheless in reasonably good agreement with the experimental data, indicating that the HX mock-ups manufactured have no significant bypass-flow.

5. Discussion of the data

Although the main purpose of the experiments is the checking of the quality of the manufacturing through the comparison of the measured to the calculated pressure drops, further data analysis is of interest for improving the understanding of the pressure drop mechanism in the zig-zag type HX-types. The established practice for pressure drop analysis is the representation of data in terms of a "friction" coefficient C_f (equ. 1),

$$C_f = \frac{\rho \Delta p A^2}{1/2\, \dot{m}^2} \qquad (1)$$

where A is the cross-section of the flow channel responsible for a majority of the pressure drop. While A is yet to be ascertained, $C_f A^{-2}$ can be directly obtained from the experimental data according to (equ.1). When plotted against ReP, where P is the wetted perimeter and Re the corresponding Reynolds number (equ. 2)

$$\mathrm{Re} = \frac{4\dot{m}}{\mu P} \tag{2}$$

the laminar and turbulent flow regimes can be clearly identified with distinct Re scaling of Re^{-1} and $\mathrm{Re}^{-\alpha}$,$\alpha \sim 0.1-0.3$. In addition, pressure drops not due to viscosity (μ), such as the surface roughness, orifices and sharp bends, add a Re independent constant friction coefficient which becomes dominant at very high Re. In figure 5, the experimental pressure drop data of TF and CC HX mock-ups (from figure 3) are presented as $C_f A^{-2}$ vs ReP. It becomes immediately evident that the CC and TF HX have similar flow characteristics. In addition the transition from laminar to turbulent flow is clearly identifiable. The nominal friction factors of CC and TF HX differ by a factor 1.8 at the same nominal Reynolds number.

At present, the experimental data lead us to the following observations. 1- a satisfactory scaling of measurements at different inlet pressures and for different gases; 2- as expected change in friction factor scaling with Reynolds number in transition from laminar to turbulent flow; 3- a consistent and similar behaviour shown by both CC and TF HX; 4- the similar friction coefficient scaling from CFD model is more likely to be significant than coincidental;

The reliability/validity of the experimental data would be considerably strengthened if the similarity in the friction coefficient *scaling* between CC and TF could be unified into a single correlation C_f(Re) with a plausible definition of flow channel geometries (A, P and D_h, the hydraulic diameter). The underlying flow geometry for a unified friction factor correlation, if it does indeed exists, must be contained within the flow passage a pair of zigzag fins, which repeats along the HX. There are two key

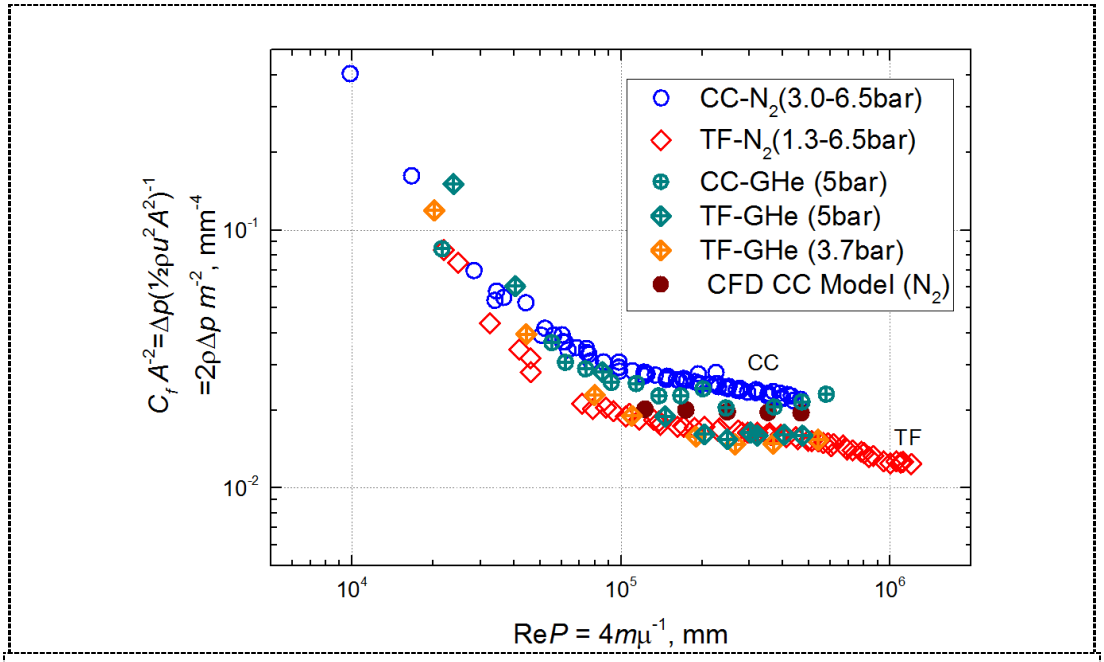

Figure 5. Nominal friction coefficient vs nominal Reynolds number for CC and TF HX

flow cross-sections, plane 1 of narrow channel flow between fins and plane 2 of a sharp U-bend for zigzag from one narrow channel to the next. In addition there is also some flow around the centre

copper core with a form drag similar to the flow across a cylinder. For unifying the nominal friction coefficient scaling of CC and TF into a common C_f(Re) correlation, the underlying flow passage geometry should yield the same critical Reynolds number for transition from laminar to turbulent flow. As shown in figure 5, the experimental data indicate the critical mass flow rate are $\dot{m}_{c,CC}$=0.3 g/s and $\dot{m}_{c,TF}$=0.4 g/s. Therefore the ratio of flow passage perimeter between TF and CC should be PTF/PCC=4/3. Since the overall diameter D of TF HX is about 1.7 times that of CC HX, the perimeter ratio of plane 2 for the U-bend zigzag flow passage between TF and CC is ~ 1.6, significantly larger than the required 4/3. Similarly the relevance of the flow around the centre copper core can also be eliminated as the perimeter ratio in this case is more than 2.4. In contrast, the perimeter ratio for the narrow channel flow passage is 1.3 and fits almost perfectly with the required 4/3. Could the narrow channels between the fins indeed be the only possible flow passage underlying a common C_f(Re) correlation? Further experiments and calculations are needed to verify this hypothesis and to explain the friction factor ratio of 1.8 and thus improve the understanding of the pressure drop in the ITER zig-zag HX designs.

6. Summary

This paper reports on the development of heat exchangers for the ITER current leads via mock-ups. Experiments to assess the quality and performance of these heat exchangers were conducted and compared to large 3D numerical models. This comparison confirms the absence of significant bypass-flow in the mock-ups, thus validating the chosen manufacturing approach. The heat exchangers for the ITER current leads are therefore now sufficiently verified to launch series production. In order to complete the theoretical understanding of the flow in the described heat exchangers, further investigation of the unified pressure drop mechanism between these different types of heat exchangers based on a common design should be conducted in the future.

Disclaimer

The views and opinions expressed herein do not necessarily reflect those of the ITER organization.

References

[1] Ballarino A 2008 *Physica Scripta* Vol **468** pp. 2142-2148
[2] Heller R, Darweschad S M, Dittrich G, Fietz W H, Fink S, Herz W, Hurd F, Kienzler A, Lingor A, Meyer I, Nöther G, Süsser M, Tanna V L, Vostner A, Wesche R, Wüchner F and Zahn G 2005 *IEEE Trans. Appl. Supercond.* **15** 1496-99
[3] Bi Y, Bauer P, Cheng Y, Devred A, Ding K, Huang X, Liu C, Lin X, Mitchell N, Sahu A, Shen G, Song Y, Wang Z, Zhang H, Yu J and Zhou T 2010 *IEEE Trans. Appl. Supercond.* **20** 1718-21
[4] Bi Y, Bauer P, Devred A, Ding K, Feng H, Gung C Y, Huang X, Liu C, Mitchell N, Ni Q, Shen G, Song Y and Zhou T 2011 *IEEE Trans Appl. Supercond.* **21** 1074-78
[5] Taylor T, Ballarino A, Bauer P, Bi Y, Devred A, Ding K, Fousasat A, Mitchell N, Shen G, Song Y, Yang Y and Zhou T 2012 *IEEE Trans Appl. Supercond.* **22** 4800304
[6] Bauer P, Ding K, Gung C Y, Ichihara T, Niu E, Shen G, Taylor T, Vertongen P and Zhou T 2013 *IEEE Trans Appl. Supercond.* **23** 4801104
[7] Zhou T 2014 *2014 SOFT*, *Fusion Engineering and Design*, In Press, Corrected Proof, Available online 16 May 2015
[8] Sitko M, Bordini B, Ballarino A, Bauer P and Devred A 2013 *IEEE Trans. Appl. Supercond.* **23** 4900805